THE JOURNAL OF PHYSICAL CHEMISTRY B

Article

pubs.acs.org/JPCB

Dark States in Ionic Oligothiophene Bioprobes—Evidence from Fluorescence Correlation Spectroscopy and Dynamic Light Scattering

Heike Hevekerl,[‡,§] Jens Wigenius,[†,§] Gustav Persson,[‡] Olle Inganäs,[†] and Jerker Widengren*[,‡]

[†]Biomolecular and Organic Electronics, Department of Applied Physics, IFM, Linköping University, SE-581 83 Linköping, Sweden

[‡]Experimental Biomolecular Physics, Department of Applied Physics, Royal Institute of Technology, SE-106 91 Stockholm, Sweden

Supporting Information

ABSTRACT: Luminescent conjugated polyelectrolytes (LCPs) can upon interaction with biological macromolecules change their luminescent properties, and thereby serve as conformation- and interaction-sensitive biomolecular probes. However, to exploit this in a more quantitative manner, there is a need to better understand the photophysical processes involved. We report studies of the conjugated pentameric oligothiophene derivative p-FTAA, which changes optical properties with different p-FTAA concentrations in aqueous buffers, and in a pH and oxygen saturation dependent manner. Using dynamic light scattering, luminescence spectroscopy and fluorescence correlation spectroscopy, we find evidence for a monomer−dimer equilibrium, for the formation of large clusters of p-FTAA in aqueous environment, and can couple aggregation to changed emission properties of oligothiophenes. In addition, we observe the presence of at least two dark transient states, one presumably being a triplet state. Oxygen was found to statically quench the p-FTAA fluorescence but also to promote molecular fluorescence by quenching dark transient states of the p-FTAA molecules. Taken together, this study provides knowledge of fluorescence and photophysical features essential for applying p-FTAA and other oligothiophene derivatives for diagnostic purposes, including detection and staining of amyloid aggregates.

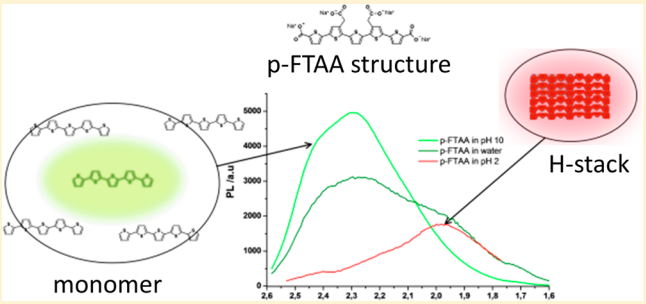

1. INTRODUCTION

The nature of the interactions between luminescent conjugated polyelectrolytes (LCPs) and biological macromolecules determines the possibilities to use LCPs as conformation- and interaction-sensitive biomolecular probes. Whereas LCPs with anionic, cationic, and zwitterionic character all can be used for these purposes, the interactions include hydrophobic $\pi-\pi$, electrostatic, and hydrogen bonding, and the balance of these may presumably vary depending on the specific LCP−biomolecule combination.[1] The probing of interactions is indirect, through the optical absorption and emission of the LCPs, but is also strongly influenced by self-aggregation, environmental, and excitation conditions, and if and to what extent the LCPs under study enter into dark states during the experiments. Such states can either be excitation-induced transient dark states (triplet, photoisomerized, photoionized, or radical states), be caused by static quenching by external compounds, or may follow as a consequence of self-quenching upon aggregation. For the use of LCPs as conformation- and interaction-sensitive probes, it is essential to be able to identify luminescence changes related to the interaction itself, and to separate them from other effects. There is thus a need to better understand the aggregation properties of LCPs, the photophysical processes involved, and how they are correlated to each other.[2]

For organic fluorophores used in biomolecular studies, light-induced triplet state formation,[3] photoinduced trans−cis isomerization,[4] ionization, and radical state formation[5,6] can readily occur. Formation of such states leads to lowered time-averaged fluorescence intensities, and can be evidenced as fluorescence blinking in, e.g., fluorescence fluctuation spectroscopy measurements.[3−6] These states are also common for LCPs in general.[7,8] Static quenching is typically the result of a complex formation between a fluorescent molecule and an external quencher. With efficient quenchers, the fluorescence is then extinguished as long as the complex exists. Dark, or dim, states can also be generated following aggregate formation, typically also generating spectral changes. LCPs often show broad bands of absorption and emission with shifts that are strongly associated with variations in their conjugation length and the coherence of excited states distributed over associated LCPs. Correlation between size measurements and emission spectra in earlier polythiophene derivatives have been difficult to interpret.[9] The reason is the polydispersity in chain length of the derivatives, which determines their number of possible conjugation length compositions and hence their luminescent

Received: February 6, 2014
Revised: April 9, 2014
Published: May 7, 2014

   dx.doi.org/10.1021/jp501324e | J. Phys. Chem. B 2014, 118, 5924−5933

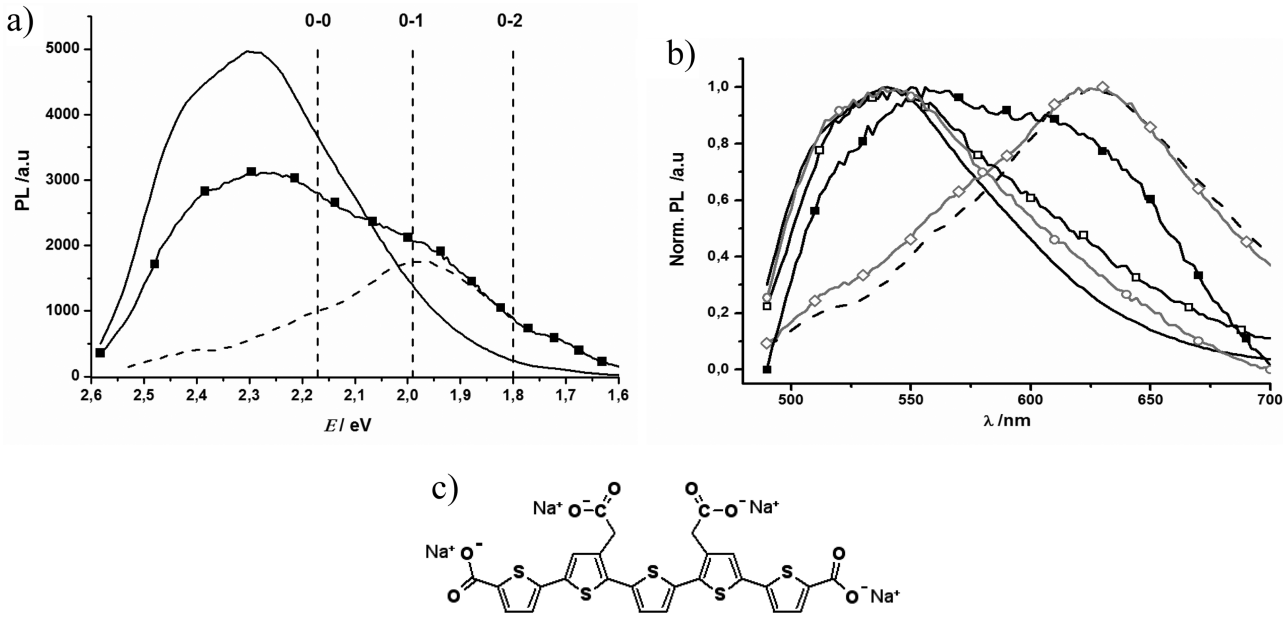

Figure 1. Photoluminescence (PL) (versus photon energy in eV) (a) and peak normalized PL (versus emission wavelength) (b) of 2 μM p-FTAA excited at 450 nm; in $NaCO_3$ (pH 10) (solid, black) (scaled down 60× in part a), HAc (pH 2) (dash, black), and mqH_2O (■, black) (scaled down 2× in part a). In part b, also 2 μM p-FTAA in mqH_2O after filtration through a 0.2 μm filter (□, black), 0.2 μM p-FTAA in mqH_2O (○, gray), 10 μM p-FTAA in mqH_2O (◇, gray). ((a) Estimated vibronic transitions marked with vertical dashed lines for p-FTAA in pH 2). (c) Chemical structure of p-FTAA.

properties. Conformation changes due to twisting and bending of the polythiophene chain affect the effective conjugation length through intrachain energy relaxation processes, while chain packing, aggregation, and/or separation of chains affect the coherence length through interchain energy relaxation processes.[1e,10] A planarization of the backbone will not only increase the conjugation length and red shift spectra[1c,11] but also affect the probability for π-stacking, and hence interchain energy relaxation and quenching.[12] π-stacked oligothiophenes are well-known to form H-aggregates whose relative oscillator strength and degree of disorder determine their vibronic structure both in absorption and in photoluminescence.[1e,10c,d] The symmetric C═C stretching results in a vibronic structure, with emission peaks commonly separated by 0.18−0.2 eV, that affects the optical spectrum. In a perfect H-aggregate, emission from a 0−0 transition is not allowed because of symmetry selection rules. However, by introducing disorder, symmetry is perturbed, and emission from the 0−0 transition will be allowed, dramatically influencing the photoluminescence (PL) spectrum, as we recently showed for the LCP tPOMT.[10d]

We here use the novel oligothiophene electrolyte, 4′,3‴-bis-carboxymethyl-quinquethiophene-dicarboxylic acid (p-FTAA) (Figure 1c) (molar mass M = 744 g·mol^{-1}). p-FTAA is monodisperse and well-defined in chain length, and therefore, we expect variations in conjugation length induced only by conformational changes, or by changes in the oligomerization or aggregation state.[14] Such changes will also affect the population dynamics of dark transient states, where the configuration of p-FTAA (Figure 1c) suggests that formation of triplet, isomerized, photoionized, and radical states in principle all can take place upon excitation. In this work, we use absorption and emission spectroscopy, dynamic light scattering (DLS), and fluorescence correlation spectroscopy (FCS) to elucidate the correlation between photophysical behavior and aggregation states of p-FTAA, and to identify what dark states and what corresponding clusters/aggregates are formed under different environmental conditions (different pH, oxygen concentrations, and presence of potassium iodide). The combination of light scattering, taking into account all objects, and FCS, where only emitting objects contribute, help to elucidate the extent to which LCPs are present in dark states, in particular in statically quenched states. As a complement, we also use FCS as a tool to characterize the population of transient dark states, as observed via the blinking behavior of the LCP compounds as they traverse through the confocal excitation/detection volume. Taken together, these analyses bring us better knowledge of the photophysical properties of p-FTAA and how they are linked to its state of aggregation. This will in turn make it easier to identify luminescence changes specifically reflecting the interplay between LCPs and biomacromolecules, and under what conditions these changes can be properly separated from other effects.

2. EXPERIMENTAL METHODS

All chemicals were used as provided by Sigma-Aldrich, Sweden, if not stated otherwise in the text. All buffers, 2 M acetic acid with 0.5 M NaCl (pH 2.0) or 100 mM sodium carbonate ($NaCO_3$) (pH 10.0), were prepared on the day of use in double distilled deionized water (18 MΩ, Milli-Q, Millipore) (mqH_2O). All buffers were filtered with a 0.2 μm PVDF syringe filter prior to use. The synthesis of p-FTAA (Figure 1c) was reported elsewhere.[2] The compound as received was dissolved in mqH_2O, subdivided into aliquots, and stored as stock solutions (2 mM) at −20 °C protected from light. The stock solutions were diluted with mqH_2O to 150 μM and when filtered (0.2 μm HAWP (Millipore) syringe filter), at the day of use. Prior to use, the sample solution was further diluted in the desired solvent to a final concentration of 2 μM, if not stated otherwise.

2.1. Photoluminescence and Absorption. All photoluminescence (PL) experiments, except deoxygenation meas-

dx.doi.org/10.1021/jp501324e | J. Phys. Chem. B 2014, 118, 5924−5933

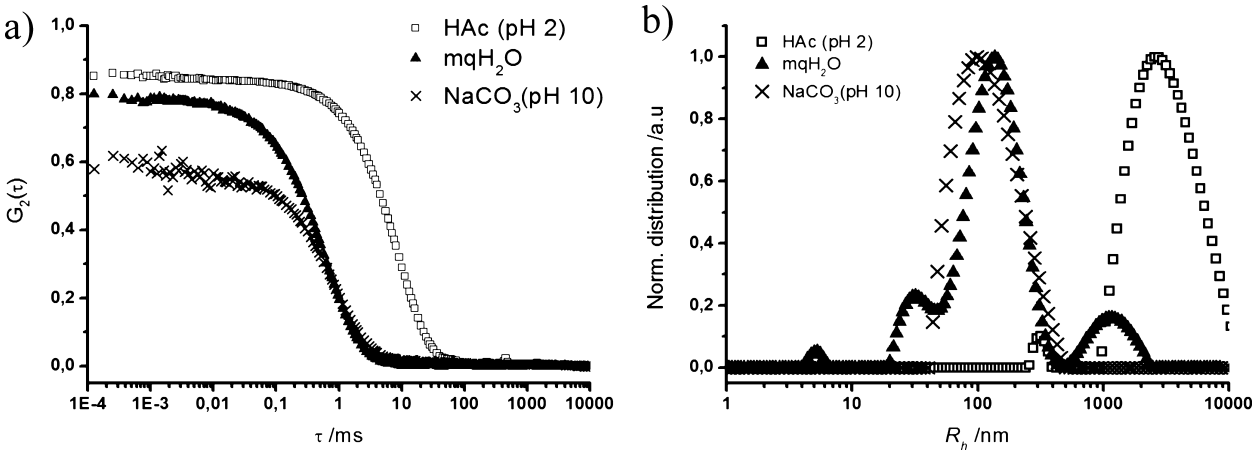

Figure 2. DLS autocorrelation functions (a) and corresponding hydrodynamic radii (R_h) (b) after CONTIN analysis, of 2 μM p-FTAA in HAc (pH 2), mqH_2O, or $NaCO_3$ (pH 10).

urements, were performed with a Safire2 plate reader (TECAN, Switzerland) using Costar 96 half width, flat bottom, black, nontreated plates (Corning, U.K.). 450 nm light was used for excitation, averaging three individual samples and compensating for buffer response. The influence of oxygen on the PL was measured with a FluoroMax-4 spectrofluorometer with time-correlated single photon counting (TCSPC) (Horiba JobinYvon, France) using 450 nm excitation light. The sample solution was placed in a quartz cuvette and thoroughly bubbled with argon to remove oxygen. A flow of argon was maintained above the sample surface during measurements to prevent oxygen from interacting with p-FTAA. The same instrument was used for fluorescence lifetime measurements in the TCSPC mode, with 495/30 nm excitation, and with emission detected at 565/18 nm.

Absorption measurements were performed with a Lambda 950 UV/VIS spectrometer (PerkinElmer, U.K.) using 1.4 mL quartz cuvettes.

2.2. Dynamic Light Scattering. The hydrodynamic radius (R_h) of p-FTAA was determined by dynamic light scattering as an average of the results of three to five individual measurements. The DLS setup, an ALV/DLS/SLS-5022 compact goniometer system (ALV Gmbh, Langen, Germany), used a HeNe laser (632.8 nm, power 22 mW) as a light source and two avalanche photo diodes (PerkinElmer, Vaudreuil, Quebec, Canada) as detectors, working in cross-autocorrelation mode. Temperature was kept constant (293.15 ± 0.05 K) in the surrounding toluene bath. The scattered light was collected at 90° from the incident laser. Intensity correlation curves were analyzed with the ALV-5000/E/EPP&ALV 60X0-win V3.0.2.3 software based on standard CONTIN analysis.[15]

2.3. Fluorescence Correlation Spectroscopy. Fluorescence correlation spectroscopy (FCS)[16] measurements were performed on two different home-built epi-illuminated confocal instruments. In both cases, a 440 nm diode laser (LDCU12/6104, Power Technology, Inc., Little Rock, AR, USA) was used for excitation. The excitation power was controlled by insertion of neutral density glass filters into the beam path. For the study of diffusion behavior in different environments, a Leitz-Wetzlar upright microscope stand was used and the sample was applied as a hanging droplet. A Zeiss 63×, NA 1.2, NeoFluar water immersion objective was used for focusing the excitation light and for fluorescence collection. The fluorescence emission was separated from the excitation light by a dichroic mirror, and a 50 μm pinhole was placed in the back focal plane to limit the axial extension of the observation volume. After the pinhole, the fluorescence was split by a 50/50-beam splitter cube, discriminated from scattered light by optical band-pass filters (HQ565/75m, Chroma Technology, Rockingham, VT, USA) and focused onto two single-photon-sensitive avalanche photodiodes (APDs, SPCM-AQR-13/14, PerkinElmer Optoelectronics, Fremont, CA, USA) in a so-called Hanbury-Brown and Twiss arrangement.[17] This arrangement, in combination with cross-correlation of the detector signals, circumvents the detector dead-time and eliminates the effects of detector afterpulsing on the correlation curves, thus enabling the use of the full time resolution of the correlator (ALV-6010/160, ALV GmbH, Langen, Germany).

Calibration measurements using a well-known emitter, Rhodamine 110 (Rh110), were first performed to align the setup and determine the properties of the observation volume. The diffusion time of Rh110, τ_D = 24.1 ± 1.3 μs, was later used as a reference to estimate the molar mass (M) of p-FTAA. To avoid setup variations, the alignment of the setup was repeatedly checked within each measurement session using this Rh110 sample as a control.

For the study of photophysical processes in the microsecond time range, longer measurements were required to achieve sufficient statistics in the correlation channels of interest. In these measurements, and for the deoxygenation experiments, an Olympus IX-70 inverted microscope stand was used to facilitate the use of closed sample containers, providing more stable measurement conditions by allowing larger sample volumes and prohibiting solvent evaporation. An Olympus 60×, NA 1.2, UplanApo objective was used in combination with a 150 mm achromat as a tube lens to focus the emission onto the pinhole, yielding an effective magnification of 50×. An ALV-5000/E correlator (ALV GmbH, Langen, Germany), with an ALV 5000/FAST Tau Extension board, was used for data acquisition. In this setup, the focus was larger, and the diffusion time for Rh110 was determined to 51 μs. p-FTAA was diluted in pH 10 buffer to a final concentration of 0.2 μM, if not stated otherwise, and placed in a sealed beaker to allow control of the surrounding atmosphere. The oxygen concentration could be reduced by gently bubbling the solution with argon or nitrogen. The average excitation irradiance in the detection volume was varied from 25 kW/cm^2 up to 300 kW/cm^2. Potassium iodide (in a series of concentrations: 1.5−10 mM) was added to

dx.doi.org/10.1021/jp501324e | J. Phys. Chem. B 2014, 118, 5924−5933

alkaline p-FTAA solution (0.3 μM) to study its effect on photophysical properties, such as singlet−triplet state kinetics and photo-oxidation.

3. RESULTS

3.1. Spectral Dependence of the Fluorescence Emission on Oligomer Concentration and Solvent pH. The fluorescence emission spectrum of p-FTAA is broad, ∼500−750 nm, and highly environment dependent. p-FTAA emitted brightly when dissolved in a highly alkaline buffer (100 mM $NaCO_3$, pH 10). The emission was ∼60 times more intense compared to when the compound was dissolved in mqH_2O or acidic buffer (2 M HAc, pH 2) (Figure 1a). Further, in pH 2 or for highly concentrated p-FTAA (10 μM) in mqH_2O, the emission peak was red-shifted by around 85 nm, from 545 to 630 nm (Figure 1b). Lowering the p-FTAA concentration in mqH_2O from 10 to 2 μM broadened the emission spectrum, blue-shifted the peak back to ∼545 nm, and gave rise to a second new shoulder around 515 nm (Figure 1b). The peak at 630 nm was not discernible after further diluting the dispersion to 0.2 μM, which made the spectrum regain a shape similar to when the compound was dissolved in pH 10 (Figure 1b). Filtration of 2 μM p-FTAA dispersions through a filter with 0.2 μm pores also blue-shifted emission spectra, removing the shoulder at 630 nm in the mqH_2O dispersion and almost extinguishing the emission of the pH 2 dispersion (Figure 1b), indicating that the peak at 630 nm originates from larger aggregates. The smaller emitters contributing to the bluish part of the spectra remained in the dispersion after filtration.

3.2. Dynamic Light Scattering. The observations after filtration in the previous part prompted us to further elucidate the fluorescence emission behavior through DLS measurements. The resulting autocorrelation curves for 2 μM p-FTAA are plotted in Figure 2a. Significant differences between the three samples were observed and confirm the previous assumptions. At pH 2, large clusters with long diffusion times were detected, corresponding to a spherical hydrodynamic radius (R_h) of 1−10 μm (Figure 2b). Filtration by a 0.2 μm filter apparently removed all or nearly all p-FTAA molecules and left no measurable scattering. When dissolved in mqH_2O, a wide R_h value span was observed, ranging from 20 to 400 nm, with a major scattering peak found around 120 nm. A population that corresponds to larger aggregates, around 1 μm in R_h, was also indicated after the CONTIN analysis. However, according to the Rayleigh approximation, the contribution from a scattering particle to the DLS correlation curves scales with the sixth power of the particle diameter. Hence, this contribution to the DLS correlation curves originates from just a few diffusing entities (Figure 2b). No significant change of the correlation curve was observed after filtration of this sample. p-FTAA dissolved in pH 10 showed a narrower aggregate size distribution, focused around 100 nm and without traces of larger aggregates. Nevertheless, it should also be noted that a small distribution peak arose around 5 nm, with mqH_2O as well as with the pH 10 buffer as solvent. Hence, the dispersion is likely to contain also single chains or clusters of p-FTAA chains. However, these small peaks were close to the detection limit, which makes them difficult to interpret. Therefore, other techniques need to be used to reach full interpretation of the DLS data. Nonetheless, due to the size dependence of the scattering intensity, the number of these very small objects in the dispersions can be quite large. In analogy with the concentration dependence of the blue-shifted PL peak in mqH_2O (Figure 1a), a concentration dependent R_h was observed throughout the DLS measurements. A reduction of R_h with around 80 nm was observed when reducing the p-FTAA concentration from 2.0 to 0.2 μM (Table 1). Also, in pH 2 solution, R_h was decreased when reducing the concentration, but still mainly large scattering clusters with R_h = 1.25 ± 0.35 μm were detected. In contrast, the R_h of p-FTAA clusters was independent of concentration when dissolved in pH 10.

Table 1. Hydrodynamic Radius of p-FTAA Clusters[a]

[p-FTAA][b] (μM)	$NaCO_3$ (pH 10)	mqH_2O	HAc (pH 2)
10.0	122 ± 37	98 ± 33	2450 ± 750
2.0	144 ± 48	100 ± 32	1450 ± 410
0.2	159 ± 58	18 ± 7	1250 ± 350

[a]In nm and full width at half-maximum (fwhm) calculated from DLS autocorrelation function in different solutions. [b]Concentration of p-FTAA.

3.3. Fluorescence Correlation Spectroscopy. Significant differences between p-FTAA samples in the three different environments were observed when examining the dispersions with FCS. In pH 2, the mean fluorescence intensity per detection channel was very low, 1.4 kHz at the excitation power used (100 kW/cm^2), and in line with the steady-state fluorescence spectroscopy measurements. A small number of slowly diffusing and weakly emitting large aggregates yielded spiking intensity traces, making it hard to interpret the results. Nevertheless, averaging of four 60 s measurements, with intensity traces selected to be free of major spikes, yielded a correlation curve (Figure 3a) that could be well fitted using a standard model for one diffusing entity and one exponential component representing, for instance, singlet−triplet state kinetics. This model is given by[3]

$$G(\tau) = \frac{\langle F(t)F(t+\tau)\rangle}{\langle F(t)\rangle^2} = G_D(\tau)\frac{1 - T + Te^{-\tau/\tau_T}}{1 - T} + 1 \quad (1)$$

Here, $F(t)$ denotes the detected fluorescence intensity at time t, square brackets denote time average, and τ denotes the correlation time. T is the average fraction of the fluorescent molecules within the detection volume residing in a dark state, e.g., a triplet state, τ_T is the average relaxation time for the dark state transitions, and $G_D(\tau)$ reflects the diffusion properties of the fluorescent species.

$$G_D(\tau) = \frac{1}{N}\left(1 + \frac{\tau}{\tau_D}\right)^{-1}\left(1 + \frac{\tau}{\beta^2\tau_D}\right)^{-1/2} \quad (2)$$

Here, N is the average number of emitting entities in the detection volume, τ_D is the average dwell time, and β is the ratio of the axial and transverse extensions of the approximately 3D-Gaussian detection volume.

In mqH_2O, we again observed weak fluorescence (5.4 kHz) correlating well with the fluorescence emission spectrum (Figure 1b), but in order to properly fit the autocorrelation curve we needed to use a model with two diffusion components,[18] which yielded a long τ_D of ∼2 ms and a short τ_D of 23 μs (Figure 3b, Table 2). This indicates the presence of both single p-FTAA molecules (or small aggregates of a few molecules) and much larger aggregates (micrometer in size). The results of this fit are very uncertain, and the short

dx.doi.org/10.1021/jp501324e | J. Phys. Chem. B 2014, 118, 5924−5933

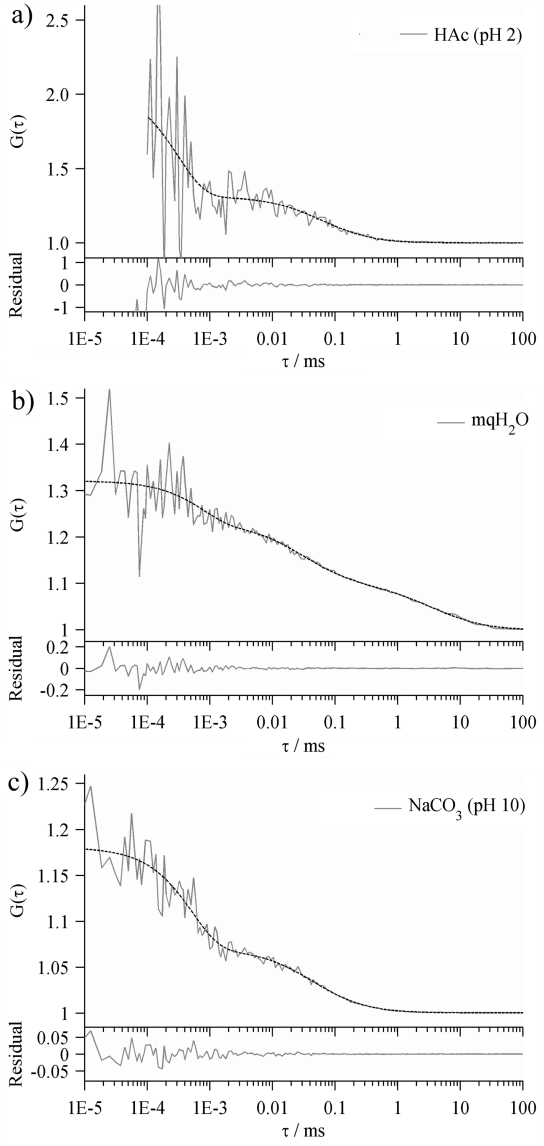

Figure 3. Experimental FCS curves (—) of 0.2 μM p-FTAA in (a) HAc (pH 2), (b) mqH_2O, and (c) $NaCO_3$ (pH 10), fitted to eq 1 (---), as described in the text. The fitting residuals are shown at the bottom. I_{exc} = 105 kW/cm^2.

Table 2. Fluorescence Correlation Spectroscopy Data of p-FTAA in Different Solutions

	N^a	$\tau_D{}^b$ (μs)	$\tau_T{}^c$ (μs)	T^d	I^e (kHz)	M (g·mol^{-1})
Rh110	0.9	24	1.9	0.01		
HAc (pH 2)	11	52	0.2	0.73	1.4	3200
mqH_2O	11	23/2000	0.5	0.39	5.4	290/26000
$NaCO_3$ (pH 10)	37	45	0.5	0.6	12	2100

[a]Number of emitting diffusing units in focus (N). [b]Diffusion time (τ_D). [c]Relaxation time of the dark state transitions (τ_T). [d]Fraction of molecules in the dark state (T). [e]Absolute intensity from the sample (I). The table data is based on measurements performed on the upright FCS setup.

relaxation time of 23 μs could be caused or biased by the presence of an additional dark transient state. However, the fluorescence signal from the sample was unfortunately neither strong nor stable enough to generate measurements allowing the introduction of more fitting parameters with meaningful results. Nevertheless, the stretched-out shape of the FCS curve (Figure 3b) indicates a wide size distribution, ranging from nanometer-sized entities to large aggregates, that is consistent with previous DLS measurements.

When measuring on p-FTAA in pH 10 (Figure 3c), we again observed an approximately monodisperse correlation function yielding a τ_D of 44.9 μs which corresponds to $M \approx 2100$ g·mol^{-1}, if applying relationship 3 to the measured diffusion times using M_0 = 331 g·mol^{-1} and τ_{D0} = 24.1 μs for Rh110 as a calibration, and disregarding any hydration effects.

$$\tau_D \propto \sqrt[3]{M} \rightarrow M = \left(\frac{\tau_D \sqrt[3]{M_0}}{\tau_{D0}}\right)^3 \quad (3)$$

Multiple measurements were performed, resulting in estimated molecular masses ranging from 1600 to 3200 g·mol^{-1} for p-FTAA (molecular weight of 744 g·mol^{-1}) diluted in pH 10. In the DLS measurements, we observed that the dispersion of p-FTAA in pH 10 contained a number of big clusters, which could not be observed to the same extent in the FCS measurements. While the contribution to the correlation curves in DLS scales with a power of 6 to the diameter of the sample particles, the contribution to the correlation curves in FCS scales only to a power of 2 with the detected fluorescence intensity from the individual particles/molecules. Moreover, the fluorescence intensity from the individual aggregates is also likely to be lower than that from a corresponding number of p-FTAA monomers, due to self-quenching effects upon aggregation.[19] Additionally, the emission filter in the FCS measurements was more suited to detect smaller oligomers than larger and red-shifted aggregates. The emission from p-FTAA in the pH 10 buffer thus originates to a large extent from single chains or small clusters containing only a few oligomers. Further, the peak at 5 nm R_h calculated for p-FTAA in pH 10 from DLS (Figure 2b) is in a similar range as the calculated τ_D and M from the FCS measurements. Similar comparisons could also be made for the mqH_2O and pH 2 dispersions. The sparse emission detected from the pH 2 sample originated mainly from monomers/oligomers or from small clusters present at a concentration below the detection limit for DLS and its resolution limit. The larger clusters seen in the DLS measurements (Figure 2) and yielding a red-shifted contribution to the fluorescence emission spectra (Figure 1a) are only seen in the FCS data as occasional spikes in the fluorescence intensity traces. These spikes generated strong distortions in the correlation curves, compared to FCS curves calculated from spike-free intensity traces. For mqH_2O, the DLS measurements indicated a lower tendency of aggregate formation than at pH 2 (Figure 2b). In the corresponding FCS measurements, the average fluorescence intensity was higher than at pH 2, and fluorescence intensity spikes from aggregates were less dominant compared to the average intensity. FCS curves could thus be recorded also in the presence of spikes without strong distortions (Figure 3b). We account the two diffusion components observed in the FCS as well as in the DLS measurements of mqH_2O to the two emission peaks observed in the corresponding emission spectrum of Figure 1b.

The FCS curve from the measurement in the pH 10 buffer (Figure 3c) clearly showed the presence of fluorescence fluctuations in the microsecond regime. A process generating such fluctuations could be, e.g., singlet−triplet state transitions,[3] trans−cis-isomerization,[4] or photo-oxidation,[5,6] i.e., the fluo-

dx.doi.org/10.1021/jp501324e | J. Phys. Chem. B 2014, 118, 5924−5933

rophore switching between the emissive state and a dark or a less detectable state. The relatively large amplitude of the component in the correlation curve pertaining to these fluctuations, around 50% of the total correlation amplitude, indicates the presence of only a single or very few independently emitting spectroscopic units in each detected diffusing unit. In large clusters, with several independently emitting spectroscopic units, the relative fluctuations introduced by the blinking of individual spectroscopic units would be smaller, compared to the fluctuations generated as the clusters diffuse into and out of the detection volume. The blinking would then generate lower relative amplitudes in the correlation curves. The large relative amplitude observed is in agreement with the observed diffusion times, which are too short to correspond to large aggregates or oligomers, and provides additional evidence that the emission in this sample occurs mainly from single chains or small oligomers. Interestingly, we note that also the FCS curves recorded from the pH 2 and mqH_2O samples display decay terms with relaxation times in the microsecond time range (Figure 3a and b). If the monomer units of the aggregates would emit and blink independently, the amplitudes of these decay terms would be too small to be detected. The relatively large amplitudes of these terms thus indicate that the emission from the monomers in the clusters/aggregates is strongly coupled.

3.4. Dark Transient States of p-FTAA. To further examine the nature of the dark state involved in the observed fluctuations at pH 10, a series of measurements with different excitation powers was performed (see the Supporting Information for details). However, the model described in eq 1 did not properly fit the correlation function in the triplet time regime. Therefore, a model assuming two independent exponential processes was applied.

$$G(\tau) = G_D(\tau)\left(\frac{1 - T + Te^{-\tau/\tau_T}}{1 - T}\right)\left(\frac{1 - U + Ue^{-\tau/\tau_U}}{1 - U}\right) + 1 \quad (4)$$

This generated significantly better fits. The relaxation times (τ_T) and the amplitudes (T) of the processes are shown in parts a and b of Figure 4, respectively. The determined parameters T and τ_T displayed an excitation power dependence typical for triplet state transitions.[3] The fraction of fluorophores in the triplet state (T) increased with increasing power, because an increased population in the excited singlet state increases the probability of a fluorophore entering the triplet state via intersystem crossing. The increased excitation rate also led to shorter measured turnover times τ_T, as expected for singlet−triplet state transitions.

The second component exhibited a more complex behavior (see the Supporting Information, Figure S1). At excitation irradiances below 100 kW/cm^2 (420 μW), it displayed a very fast process, with relaxation times of a few hundred nanoseconds. For higher excitation powers, the model fit placed this process in the diffusion regime around 60 μs, and presented a behavior similar to that expected from a photoinduced isomerization—decreasing relaxation times and an essentially unaffected fraction U with increasing excitation irradiances.[4] However, the two-component model curve fits, in the power range above 100 kW/cm^2, also showed an increase in diffusion time with increasing power followed by a final decrease for the very highest powers. This can be explained by fluorescence saturation, due to substantial triplet population

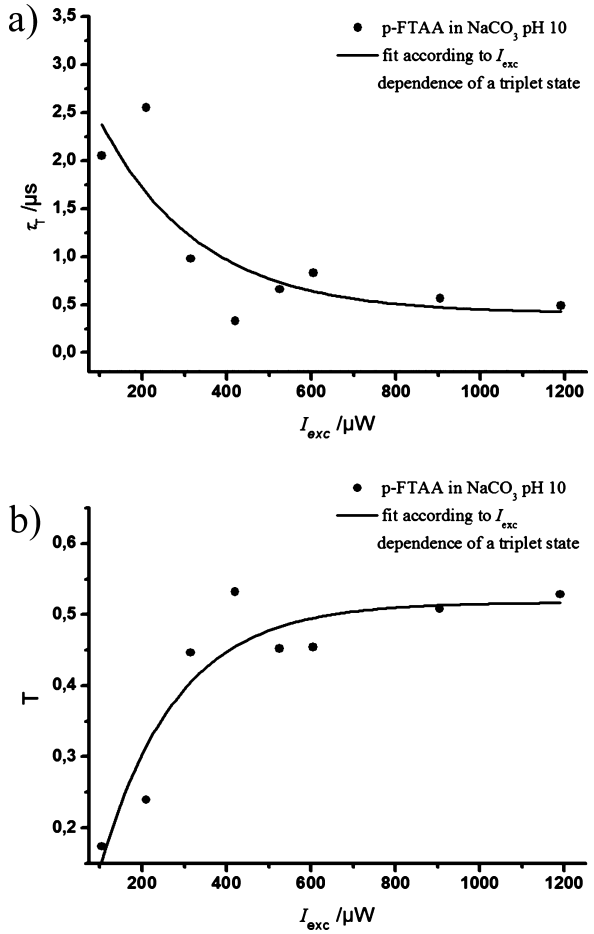

Figure 4. (a) Dependence of the relaxation time (τ_T) and (b) the relative amplitude (T) in recorded FCS curves from the p-FTAA sample dissolved in pH 10 on the applied excitation power (I_{exc}). The FCS curves were analyzed according to the two-component model of eq 4. The set of determined τ_T and T parameters were fitted to the I_{exc} dependence of the corresponding parameters for a triplet state.

build-up, affecting the spatial fluorescence intensity distribution and thereby the apparent detection volume.[3,20] At the highest powers, the saturation effect is probably overtaken by photobleaching which would in turn explain the decrease in reported diffusion time. In this context, it is not unlikely that the U component is an artifact, caused by the fitting algorithm trying to improve the fit to the diffusion part of the autocorrelation function, since the applied model does not include the aforementioned saturation effect. Nevertheless, it seems like a two-component system is not enough to completely describe the behavior of the system over the whole power series.

3.5. Effects on the Dark Transient States from Potassium Iodide and by Deoxygenation. The dark state could also be evidenced through interaction with other chemical species influencing triplet states, one being potassium iodide (KI). KI is well-known to facilitate intersystem crossing (ISC),[21] thus affecting the fraction of triplet states and their turnover rate. Depending on the energy levels of the actual system, KI could predominantly increase the rate of intersystem crossing either into or back from the triplet state, thus either increasing or decreasing the triplet state population.[22] Charge transfer from the excited dye to I^- is not expected; however, charge transfer between excited thiophene dyes and the redox

dx.doi.org/10.1021/jp501324e | J. Phys. Chem. B 2014, 118, 5924−5933

couple I^-/I^{3-} has been reported in dye sensitized solar cells.[23] However, for p-FTAA, only a minor difference was observed in the dark state relaxation part (parameters T and τ_T) of the recorded FCS curves upon addition of KI (see the Supporting Information, Figure S2 and Table S1), and the presence of KI did not affect the absorption or fluorescence emission spectra.

Oxygen is another well-known triplet state quencher. In an oxygen-free environment, molecules are expected to remain in the triplet state for longer times, leading to an increased relaxation time τ_T, triplet fraction T, and a concomitant decrease in PL intensity. However, this was not observed when oxygen was removed from the p-FTAA pH 10 solution. Instead, the amplitudes of the FCS correlation curves were decreased by up to a factor of 25, while the recorded total fluorescence intensity increased by approximately 30% (Figure 5). According

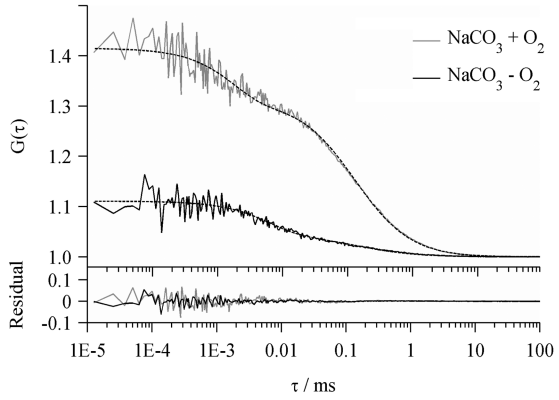

Figure 5. Experimental (gray —) and fitted (---) FCS curve of p-FTAA in $NaCO_3$ buffer (pH 10) with corresponding residuals. Upon removal of oxygen, the correlation amplitude decreases up to 25 times, corresponding to an increase in the number of fluorescent units by the same factor (black —). I_{exc}: 200 kW/cm^2.

to eq 2, this would indicate an up to 25-fold increase in the concentration of diffusing fluorescent units in the sample, and the PL intensity per diffusing unit/molecule (counts per molecule, CPM) would then decrease to almost the same extent.

One possible reason for this observation could be that molecular oxygen promotes p-FTAA oligomerization, and that upon removal of oxygen the p-FTAA oligomers would dissociate. To test this hypothesis, FCS measurements of p-FTAA in pH 10 buffer were performed, with and without addition of the detergent Triton X-100 (1%, volume). In the presence of Triton X-100, the recorded average number of freely diffusing fluorescent units in the detection volume (N) showed a distinct increase (Figure 6). PEG treated cover glasses,[24] could be used to eliminate an increase in the number of freely diffusing p-FTAA units, originating from p-FTAA stuck to the microscope cover glass being dissolved from the glass by Triton X-100. The increase in N was then found to be close to a factor of 2, at p-FTAA concentrations in the range 100−400 nM, and somewhat less than 2 in the nM range. This indicates that p-FTAA is predominantly in a dimer form in the 100 nM range, and that the presence of oxygen at least does not seem to promote the generation of any larger oligomers.

Further, the concentration dependence of τ_D, CPM, T, and τ_T for p-FTAA was investigated. With increasing concentrations, a minor increase in τ_D could be observed (Figure 7A), well in agreement with the difference in τ_D expected between a

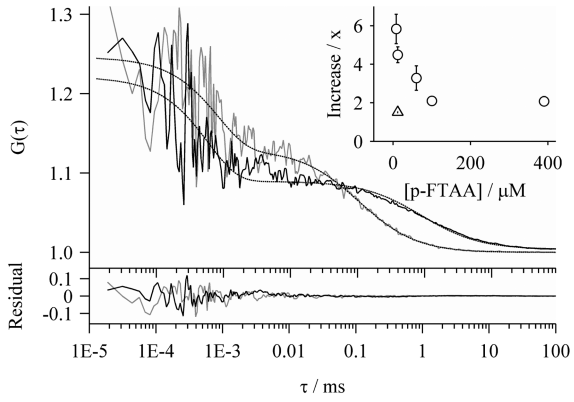

Figure 6. Experimental (gray —) and fitted (---) FCS curve of p-FTAA in $NaCO_3$ buffer (pH 10) with corresponding residuals. The coverslip is PEG-coated to avoid absorption of p-FTAA to the glass. Upon addition of the detergent Triton X-100 (1% volume), the average number of freely diffusing fluorescent units, N, in the detection volume is increased by a factor ≈2 (black —) and the diffusion time, τ_D, is prolonged due to micelle formation around single p-FTAA molecules. Inset: Factorial increase in N upon addition of Triton X-100, shown for different concentrations of p-FTAA. The pronounced increase in N at nM concentrations is due to the dissolution of p-FTAA from uncoated glass surfaces (○) and is not observed for PEG-coated glass surfaces (△). I_{exc}: 90 kW/cm^2.

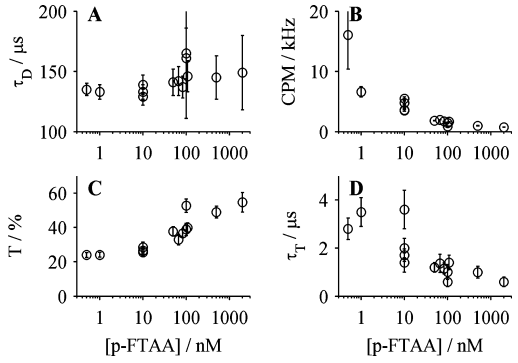

Figure 7. Concentration dependence of the diffusion time (τ_D, A), the fluorescence count rate per molecule (CPM, B), the triplet state fraction (T, C), and the triplet state relaxation time (τ_T, D) of p-FTAA in $NaCO_3$ (pH 10) buffer, as obtained from FCS measurements. Errors represent the 95% confidence interval of the fitted parameter. I_{exc}: 200 kW/cm^2.

monomer and a dimer of p-FTAA (eq 3). CPM decreased by about an order of magnitude (Figure 7B), T increased from 20% to above 50% at the excitation intensity used (Figure 7C), and τ_T decreased by about a factor of 5 (from 4 μs to less than 1 μs, Figure 7D). The higher levels of T observed for higher p-FTAA concentrations indicate that the dimers undergo singlet−triplet transitions in concert as one unit, not as two independently blinking monomers. Moreover, together with the shorter τ_T observed for higher concentrations, the higher T levels indicate that the intersystem crossing rates are higher for the dimers than for the monomers.

To further understand the role of oxygen in the observation of Figure 5, emission spectra and fluorescence lifetime measurements of N_2 and air-saturated pH 10 solutions of p-FTAA were recorded and compared. No differences in the fluorescence lifetimes or in the normalized emission spectra in the absence or presence of oxygen could be observed

dx.doi.org/10.1021/jp501324e | J. Phys. Chem. B 2014, 118, 5924−5933

(Supporting Information, Figures S3 and S4). This indicates that the fluorescence properties of the emissive states of p-FTAA, i.e., its ground and excited singlet state, are unaffected by molecular oxygen.

4. DISCUSSIONS

In this study, we have investigated the aggregation and dark transient state properties of p-FTAA by a combination of spectrofluorometry, DLS and FCS. The interpretation of the experiments is summarized in Figure 8 and is further discussed below.

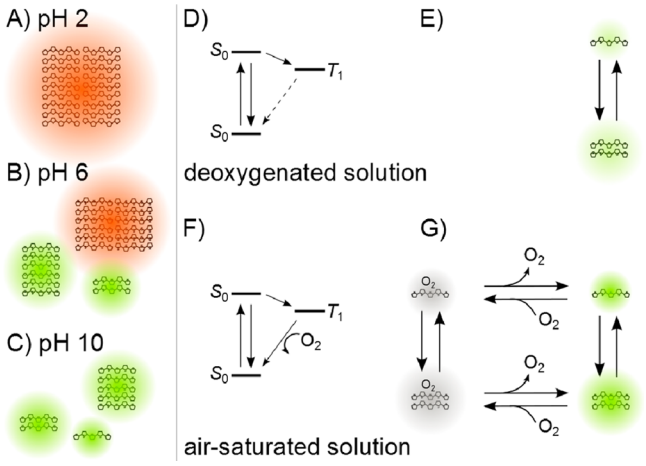

Figure 8. (A–C) Observed states of aggregation and cluster formation of p-FTAA. At pH 2 large and weakly associated clusters of rather well-ordered H-aggregates with red-shifted emission are found (A), in the mqH_2O dispersion we observe a mixture of small emitters and large weakly associated H-aggregates (B), while in the pH 10 solution we observe emission from fully dissolved single chains or tiny aggregates containing only a few oligothiophene chains (C). (D–G) Major effects of oxygen on p-FTAA fluorescence. On the one hand, oxygen promotes fluorescence by quenching the dark triplet state, T_1 (F). In the absence of oxygen, the triplet state deactivation is very slow (dashed line in part D), which can result in a strong accumulation in the T_1 state. On the other hand, oxygen can also form reversible charge transfer complexes with p-FTAA (G). Thereby, a considerable fraction of the p-FTAA molecules are statically quenched in air-saturated aqueous solutions.

4.1. PL Spectra and Their Relation to Aggregation States. It can be noted that oligothiophenes are well-known to form H-type aggregates with vibronic transitions, separated by the C=C stretching characteristic 0.18–0.2 eV,[10c,13b] as we previously demonstrated for the LCP tPOMT. Accordingly, in the spectrofluorometry data (Figure 1a and b), the PL spectrum of the pH 2 dispersion can be qualitatively treated to be a result of H-type aggregation (Figure 8A). With the 0–0 transition forbidden in well-ordered H-aggregates, the most intense peak around 620 nm = 2.0 eV can be assigned to the 0–1 transition. The peak also appears in mqH_2O (Figure 8B), while it is absent in the pH 10 solution (Figure 8C). The 0–0 transition (570 nm = 2.18 eV) is not fully extinguished in pH 2, indicating some disorder in the aggregates. This is supported by FCS measurements, where huge clusters, detected as large spikes in the intensity traces strongly distorting the FCS curves, were found, together with small and weakly emitting diffusing units. The latter were not detectable with DLS but could be analyzed by FCS for spike free intensity traces (Figure 3a). Weak emission is also expected from H-aggregates because of self-quenching and interchain relaxation processes.[19] For the mqH_2O samples, PL spectra (Figure 1a and b), DLS (Figure 2), and FCS data (Figure 3b) all indicate somewhat smaller and more weakly emitting H-aggregates than for the pH 2 dispersion, coexisting with smaller clusters, oligomers, or even single monomers. The PL spectrum from p-FTAA dissolved in pH 10, however, cannot be interpreted as caused by H-aggregation. Considering the short diffusion time found in the FCS measurements (Figure 3c), similar to what is expected for single p-FTAA or tiny clusters, we conclude this dispersion to be a representation of single emitters, largely undetectable by DLS measurements. Neither is it possible to fully reconstruct the PL from p-FTAA dissolved in mqH_2O using only spectra due to H-aggregation. However, after subtracting the pH 2 spectrum from the mqH_2O spectrum, assuming that the former represents large aggregates, and normalizing, the result coincides with the normalized spectrum of p-FTAA in pH 10, i.e., that originating from single emitting p-FTAA molecules (Figure 9). We therefore conclude that the emission in pH 2

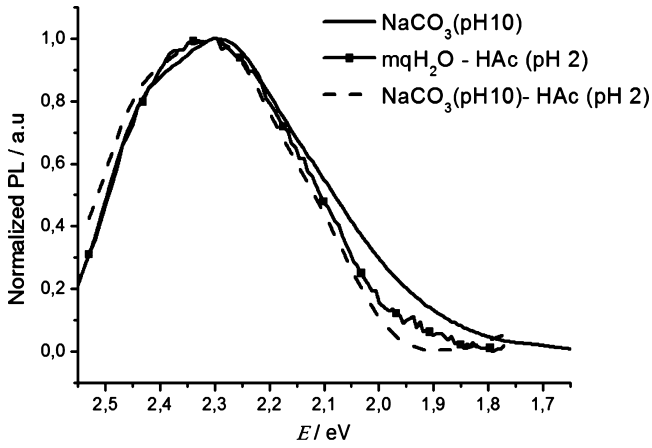

Figure 9. Normalized photoluminescence spectrum of p-FTAA in pH 10 compared to the spectra acquired for p-FTAA in pH 10 and mqH_2O after subtracting the spectrum of p-FTAA in pH 2.

originates from large and weakly associated clusters of rather well-ordered H-aggregates (Figure 8A), in the mqH_2O dispersion from a mixture of small emitters and large weakly associated H-aggregates (Figure 8B), while in pH 10 the emission originates from fully dissolved single chains or tiny aggregates containing only a few oligothiophene chains (Figure 8C).

4.2. Dark Transient States of p-FTAA and Effects of Oxygen. From the FCS measurements, in the pH 2, pH 10, as well as the mqH_2O solution (Figure 3), we found that a large fraction of LCPs are in a dark transient state. LCPs can most adequately be used as interaction- and conformation-sensitive probes when in a monomeric or dimeric form, rather than in larger clusters or aggregates. We therefore more closely investigated the transient state properties of p-FTAA in the pH 10 buffer. Although at least one more fast process seems to contribute to the dark state, which further complicates the data interpretation, we can from the excitation power dependence conclude that the transient state is largely attributed to a triplet state. Interestingly, however, upon oxygen removal, and in contrast to what would be observed for most standard fluorophores, the number of emitters in the sample strongly

dx.doi.org/10.1021/jp501324e | J. Phys. Chem. B 2014, 118, 5924–5933

increases, while the total fluorescence intensity marginally increases (Figure 5). Previous studies have shown that oxygen can form a reversible charge transfer complex with polythiophenes, which quenches PL much more effectively, up to 50%, than what could maximally be achieved from Stern–Volmer collision quenching at relevant oxygen concentrations (~10%).[25] A large number of statically quenched p-FTAA chains in the dispersion would then rather be expected. Our data confirm these expectations. Static quenching of p-FTAA by oxygen can explain why the number of fluorescent molecules, observed via the parameter N in the FCS measurements (eq 2), increases when oxygen is removed (Figure 5). Another hypothesis could be that oxygen is involved in the oligomerization of p-FTAA, and that removal of oxygen would dissolve p-FTAA oligomers into monomers, thereby increasing N. However, upon oxygen removal, N was found to increase by up to a factor of 25, far higher than the 2-fold increase observed when the detergent Triton X-100 was added (Figure 6). It is not likely that oxygen would sustain complex formation in the presence of this detergent to that extent. Instead, the observed decrease in the average CPM, in combination with the observed increase in the total fluorescence intensity upon oxygen removal, can be explained by a combination of effects. (i) Formation of charge transfer complexes between p-FTAA and oxygen may change the balance between monomers and dimers of p-FTAA in the sample (Figure 8E and G). Since monomers were found to be brighter than dimers, this would change the average CPM detected. (ii) The overall recorded CPM is influenced by two opposing mechanisms. On the one hand, the fluorescence will increase by removal of the static quenching of oxygen. On the other hand, the CPM will decrease due to higher T levels, when oxygen no longer quenches the dark triplet state of p-FTAA (Figure 8D compared to Figure 8F). For monomers and dimers, the relative effect on their CPM can be different. For dimers, the triplet quenching of oxygen may have a lower effect, since the triplet states may be quenched by additional mechanisms such as $T-T$ annihilation, not present in the monomers. In FCS measurements, the relative CPM, or "detectability" of dimers compared to monomers, would then be higher in the absence than in the presence of oxygen. The dimers would then also give a larger relative contribution to the average CPM recorded in the oxygen-free FCS measurements.

The fact that both the normalized PL spectrum and the fluorescence lifetime of the sample is independent of whether oxygen is present or not confirms that the emissive singlet state of p-FTAA is not affected by oxygen, and that the observed effects upon oxygen removal indeed can be explained by a combination of opposing effects, attributed to static quenching of p-FTAA by oxygen and oxygen quenching of the triplet state of p-FTAA, both effects affecting monomers and dimers of p-FTAA to different extents. As discussed above, the quenched PL after oxygen admission is consistent with the literature on polythiophenes.

5. CONCLUSIONS

From a combination of spectrofluorometry, DLS, and FCS data, we can conclude that the emission from p-FTAA in the pH 2 sample originates from large and weakly associated clusters of rather well-ordered H-aggregates, in the mqH_2O dispersion from a mixture of small emitters and large weakly associated H-aggregates, while in pH 10 the emission originates from fully dissolved single chains or tiny aggregates containing only a few oligothiophene chains. Dark transient states could be observed in the FCS measurements for all samples, indicating that the emission from individual monomers in the large aggregates is strongly coupled to each other. The most adequate form for an LPC to act as an interaction/conformation-sensitive probe is in its monomer or dimer form. For p-FTAA at pH 10, when in its monomer–dimer form, the major dark transient state observed could be assigned to a triplet state. Oxygen was found to act as a potent static quencher of p-FTAA. However, at the same time, it also promotes photoluminescence by quenching the dark triplet state. The influence of these effects can be different on the monomer and dimer species of p-FTAA, and also the monomer–dimer equilibrium may be influenced by oxygen complex formation.

Taken together, the characterized aggregation and photophysical properties of p-FTAA can serve as a reference for other LCPs and their use as conformation- and interaction-sensitive probes. By increased knowledge about LCP aggregation, and about how aggregation properties and photophysical properties influence the luminescence changes, the particular changes related to the interactions to be monitored can be better identified and analyzed.

■ ASSOCIATED CONTENT

Supporting Information

Detailed description and FCS spectrum of the power series measurement, as well as emission spectra and fluorescence lifetime measurements with and without oxygen. This material is available free of charge via the Internet at http://pubs.acs.org.

■ AUTHOR INFORMATION

Corresponding Author

*E-mail: jwideng@kth.se.

Author Contributions

§Contributed equally.

Notes

The authors declare no competing financial interest.

■ ACKNOWLEDGMENTS

The authors wish to thank Dr. K. Peter R. Nilsson and Dr. Andreas Åslund, Linköping University, for kindly supplying the p-FTAA and Fredrik Bäcklund, Linköping University, for carrying out complementary DLS experiments. This study was supported by the Swedish Science Council (VR), and the Strategic Research Foundation (SSF) through the center for organic bioelectronics (OBOE), and funds from Knut and Alice Wallenberg Foundation (KAW 2011.0218).

■ REFERENCES

(1) (a) Charych, D. H.; Nagy, J. O.; Spevak, W.; Bednarski, M. D. Direct Colorimetric Detection of a Receptor-Ligand Interaction by a Polymerized Bilayer Assembly. *Science* **1993**, *261*, 585–588. (b) Nilsson, K. P. R.; Inganas, O. Chip and Solution Detection of DNA Hybridization Using a Luminescent Zwitterionic Polythiophene Derivative. *Nat. Mater.* **2003**, *2*, 419–U10. (c) Faid, K.; Leclerc, M. Responsive Supramolecular Polythiophene Assemblies. *J. Am. Chem. Soc.* **1998**, *120*, 5274–5278. (d) Gaylord, B. S.; Heeger, A. J.; Bazan, G. C. DNA Hybridization Detection with Water-Soluble Conjugated Polymers and Chromophore-Labeled Single-Stranded DNA. *J. Am. Chem. Soc.* **2003**, *125*, 896–900. (e) Wigenius, J.; Björk, P.; Hamedi, M.; Aili, D. Supramolecular Assembly of Designed α-Helical Polypeptide-Based Nanostructures and Luminescent Conjugated

Polyelectrolytes. *Macromol. Biosci.* **2010**, *10*, 836−841. (f) Tang, H.; Xing, C.; Liu, L.; Yang, Q.; Wang, S. Synthesis of Amphiphilic Polythiophene for Cell Imaging and Monitoring the Cellular Distribution of a Cisplatin Anticancer Drug. *Small* **2011**, *7*, 1464−1470. (g) Berg, I.; Nilsson, K. P. R.; Thor, S.; Hammarström, P. Efficient Imaging of Amyloid Deposits in Drosophila Models of Human Amyloidoses. *Nat. Protoc.* **2010**, *5*, 935−944. (h) Feng, X. L.; Liu, L. B.; Wang, S.; Zhu, D. B. Water-Soluble Fluorescent Conjugated Polymers and Their Interactions with Biomacromolecules for Sensitive Biosensors. *Chem. Soc. Rev.* **2010**, *39*, 2411−2419. (i) Preat, J. P. J.; Zanuy, D.; Perpete, E. A.; Aleman, C. Binding of Cationic Conjugated Polymers to DNA: Atomistic Simulations of Adducts Involving the Dickerson's Dodecamer. *Biomacromolecules* **2011**, *12*, 1298−1304.

(2) (a) Thomas, S. W.; Joly, G. D.; Swager, T. M. Chemical Sensors Based on Amplifying Fluorescent Conjugated Polymers. *Chem. Rev.* **2007**, *107*, 1339−1386. (b) Herland, A.; Inganäs, O. Conjugated Polymers as Optical Probes for Protein Interactions and Protein Conformations. *Macromol. Rapid Commun.* **2007**, *28*, 1703−1713. (c) Nilsson, K. P. R. Small Organic Probes as Amyloid Specific Ligands - Past and Recent Molecular Scaffolds. *FEBS Lett.* **2009**, *583*, 2593−2599.

(3) Widengren, J.; Mets, Ü.; Rigler, R. Fluorescence Correlation Spectroscopy of Triplet States in Solution - a Theoretical and Experimetnal Study. *J. Phys. Chem.* **1995**, *99*, 13368−13379.

(4) Widengren, J.; Schwille, P. Characterization of Photoinduced Isomerization and Back-Isomerization of the Cyanine Dye Cy5 by Fluorescence Correlation Spectroscopy. *J. Phys. Chem. A* **2000**, *104*, 6416−6428.

(5) Widengren, J.; Chmyrov, A.; Eggeling, C.; Löfdahl, P.-A.; Seidel, C. A. M. Strategies to Improve Photostabilities in Ultrasensitive Fluorescence Spectroscopy. *J. Phys. Chem. A* **2007**, *111*, 429−440.

(6) Widengren, J.; Dapprich, J.; Rigler, R. Fast Interactions between Rh6G and dGTP in Water Studied by Fluorescence Correlation Spectroscopy. *Chem. Phys.* **1997**, *216*, 417−426.

(7) Turro, N. J.; Ramamurthy, V.; Scaiano, J. C. *Principles of Molecular Photochemistry*; University Science Books: Sausalito, CA, 2009.

(8) Birks, J. B. *Photophysics of aromatic molecules*; Wiley Interscience: London, 1970.

(9) (a) Åslund, A.; Herland, A.; Hammarström, P.; Nilsson, K. P. R.; Jonsson, B.-H.; Inganäs, O.; Konradsson, P. Studies of Luminescent Conjugated Polythiophene Derivatives: Enhanced Spectral Discrimination of Protein Conformational States. *Bioconjugate Chem.* **2007**, *18*, 1860−1868. (b) Wigenius, J.; Persson, G.; Widengren, J.; Inganäs, O. Interactions Between a Luminescent Conjugated Oligoelectrolyte and Insulin During Early Phases of Amyloid Formation. *Macromol. Biosci.* **2011**, *11*, 1120−1127.

(10) (a) Inganäs, O.; Salaneck, W. R.; Österholm, J.-E.; Laakso, J. Thermochromic and Solvatochromic Effects in Poly(3-hexylthiophene). *Synth. Met.* **1988**, *22*, 395−406. (b) Brédas, J. L.; Street, G. B.; Thémans, B.; André, J. M. Organic Polymers Based on Aromatic Rings (Polyparaphenylene, Polypyrrole, Polythiophene): Evolution of the Electronic Properties as a Function of the Torsion Angle Between Adjacent Rings. *J. Chem. Phys.* **1985**, *83*, 1323−1329. (c) Spano, F. C.; Clark, J.; Silva, C.; Friend, R. H. Determining Exciton Coherence From The Photoluminescence Spectral Line Shape in Poly(3-hexylthiophene) Thin Films. *J. Chem. Phys.* **2009**, *130*, 10.1063/1.3076079;. (d) Björk, P.; Thomsson, D.; Mirzov, O.; Wigenius, J.; Inganäs, O.; Scheblykin, I. G. Oligothiophene Assemblies Defined by DNA Interaction: From Single Chains to Disordered Clusters. *Small* **2009**, *5*, 96−103.

(11) (a) Kim, J.; Swager, T. M. Control of Conformational and Interpolymer Effects in Conjugated Polymers. *Nature* **2001**, *411*, 1030−1034. (b) Wigenius, J.; Andersson, M. R.; Esbjörner, E. K.; Westerlund, F. Interactions Between a Luminescent Conjugated Polyelectrolyte and Amyloid Fibrils Investigated with Flow Linear Dichroism Spectroscopy. *Biochem. Biophys. Res. Commun.* **2011**, *408*, 115−119.

(12) (a) Langeveld-Voss, B. M. W.; Janssen, R. A. J.; Meijer, E. W. On the Origin of Optical Activity in Polythiophenes. *J. Mol. Struct.* **2000**, *521*, 285−301. (b) Nilsson, K. P. R.; Andersson, M. R.; Inganäs, O. Conformational Transitions of a Free Amino-Acid-Functionalized Polythiophene Induced by Different Buffer Systems. *J. Phys.: Condens. Matter* **2002**, *14*, 10011−10020. (c) Berggren, M.; Bergman, P.; Fagerström, J.; Inganäs, O.; Andersson, M.; Weman, H.; Granström, M.; Stafström, S.; Wennerström, O.; Hjertberg, T. Controlling Inter-Chain and Intra-Chain Excitations of a Poly(thiophene) Derivative in Thin Films. *Chem. Phys. Lett.* **1999**, *304*, 84−90.

(13) (a) Spano, F. C. Modeling Disorder in Polymer Aggregates: The Optical Spectroscopy of Regioregular Poly(3-hexylthiophene) Thin Films. *J. Chem. Phys.* **2005**, *122*, 234701. (b) Clark, J.; Silva, C.; Friend, R. H.; Spano, F. C. Role of Intermolecular Coupling in the Photophysics of Disordered Organic Semiconductors: Aggregate Emission in Regioregular Polythiophene. *Phys. Rev. Lett.* **2007**, *98*, 206406.

(14) Åslund, A.; Sigurdson, C. J.; Klingstedt, T. s.; Grathwohl, S.; Bolmont, T.; Dickstein, D. L.; Glimsdal, E.; Prokop, S.; Lindgren, M.; Konradsson, P.; Holtzman, D. M.; Hof, P. R.; Heppner, F. L.; Gandy, S.; Jucker, M.; Aguzzi, A.; Hammarström, P.; Nilsson, K. P. R. Novel Pentameric Thiophene Derivatives for In Vitro and In Vivo Optical Imaging of a Plethora of Protein Aggregates in Cerebral Amyloidoses. *ACS Chem. Biol.* **2009**, *4*, 673−684.

(15) Provencher, S. W. A Constrained Regularization Method for Inverting Data Represented by Linear Algebraic or Integral Equations. *Comput. Phys. Commun.* **1982**, *27*, 213−227.

(16) (a) Magde, D.; Elson, E. L.; Webb, W. W. Fluorescence Correlation Spectroscopy. II. An Experimental Realization. *Biopolymers* **1974**, *13*, 29−61. (b) Rigler, R.; Mets, Ü.; Widengren, J.; Kask, P. Fluorescence Correlation Spectroscopy with High Count Rate and Low Background: Analysis of Translational Diffusion. *Eur. Biophys. J.* **1993**, *22*, 169−175.

(17) Hanbury- Brown, R.; Twiss, R. Q. Correlation Between Photons in Two Coherent Beams of Light. *Nature* **1956**, *177*, 27−29.

(18) Krichevsky, O.; Bonnet, G. Fluorescence Correlation Spectroscopy: the Technique and its Applications. *Rep. Prog. Phys.* **2002**, *65*, 251−297.

(19) Al Attar, H. A.; Monkman, A. P. Effect of Surfactant on FRET and Quenching in DNA Sequence Detection using Conjugated Polymers. *Adv. Funct. Mater.* **2008**, *18*, 2498−2509.

(20) Gregor, I.; Patra, D.; Enderlein, J. Optical Saturation in Fluorescence Correlation Spectroscopy under Continuous-Wave and Pulsed Excitation. *ChemPhysChem* **2005**, *6*, 164−170.

(21) Kasha, M. Collisional Perturbation of Spin-Orbital Coupling and the Mechanism of Fluorescence Quenching. *J. Chem. Phys.* **1952**, *20*, 71−74.

(22) Chmyrov, A.; Sandén, T.; Widengren, J. Iodide as a Fluorescence Quencher and Promoter-Mechanisms and Possible Implications. *J. Phys. Chem. B* **2010**, *114*, 11282−11291.

(23) Tan, S. X.; Zhai, J.; Fang, H. J.; Jiu, T. G.; Ge, J.; Li, Y. L.; Jiang, L.; Zhu, D. B. Novel Carboxylated Oligothiophenes as Sensitizers in Photoelectric Conversion Systems. *Chem.—Eur. J.* **2005**, *11*, 6272−6276.

(24) Hassler, K.; Rigler, P.; Blom, H.; Rigler, R.; Widengren, J.; Lasser, T. Dynamic Disorder in Horseradish Peroxidase Observed with Total Internal Reflection Fluorescence Correlation Spectroscopy. *Opt. Express* **2007**, *15*, 5366−5375.

(25) Abdou, M. S. A.; Orfino, F. P.; Son, Y.; Holdcroft, S. Interaction of Oxygen with Conjugated Polymers: Charge Transfer Complex Formation with poly(3-alkylthiophenes). *J. Am. Chem. Soc.* **1997**, *119*, 4518−4524.